An Examination of the δ Scuti Variable

GW Draconis from 20 years of data

Jared Davidson

A senior thesis submitted to the faculty of
Brigham Young University
in partial fulfillment of the requirements for the degree of

Bachelor of Science

Eric Hintz, Advisor

Department of Physics and Astronomy

Brigham Young University

April 2021

ABSTRACT

An Examination of the δ Scuti Variable
GW Draconis from 20 years of data

Jared Davidson
Department of Physics and Astronomy, BYU
Bachelor of Science

The δ Scuti variable star GW Draconis was found to be variable by the *Hipparcos* satellite in 1997. Since that time of discovery, it has only been examined a few times. Its high declination and short period make it a valuable target for variable star research, allowing for observations over a larger portion of the year that can capture multiple periods. We took observations from 2000 to 2020 and reprocessed this data to corroborate findings from previous papers. From 37 nights of photometric data, we determined GW Dra to have a period of 0.126186 days. Others have reported periods of 0.2545 and 0.1262 d. Frequency analysis yielded several unique frequencies and some subharmonics, but no harmonics of orders higher than the fundamental. Spectroscopic analysis shows GW Dra is an A8 or A9 star and does not indicate the presence of a stellar companion. From our data it is clear that GW Dra is multiperiodic.

Keywords: senior thesis, undergraduate research

ACKNOWLEDGMENTS

I acknowledge the Brigham Young University Department of Physics and Astronomy for its support of my research efforts. I would also like to acknowledge the many BYU students and professors that have lent their efforts in observing GW Dra throughout the last 20 years. I wish to thank my advisor Dr Eric Hintz for his help and guidance throughout my undergraduate research. I also wish to thank my lovely wife Alyssa for her love and continued support for my educational and professional goals.

Contents

List of Figures

List of Tables

Chapter 1

Background

1.1 Motivations

Variable star study is an ongoing field of research to better understand the inner workings of stars. Stars drive the evolution of galaxies and the cosmos by fusing hydrogen and helium into heavier elements. These elements are also necessary for planet formation and the creation of life. Variable star research is important because it allows us to derive information on the properties of stars that would otherwise be impossible to obtain. We are able to learn about the mass, radius, luminosity, temperature, internal and external structure, composition, and evolution of stars through careful variable star study. The long-term behavior of variable stars can be determined through continual observations over several years. Thus, variable stars play a crucial role in our understanding of the universe (Percy Accessed March 3, 2021).

GW Dra is a valuable target for variable star research. Though seldom studied, its high declination and short period allow for observations over a larger portion of the year that can capture multiple periods. Taking advantage of this fact, we observed GW Dra at Brigham Young University over the course of 20 years, covering from 2000 to 2020, to further characterize the star.

While I certainly cannot take credit for observations that were taken before I arrived at BYU (much less those that were taken before I was even in grade school), my personal contribution to the 20 year campaign has been to finish the long-standing project. It has been my task to roundup the 20 years of observations, analyze the data, and see what we can conclude about GW Dra.

1.2 Relevant Astronomy Terms

Before continuing, it is necessary to define relevant astronomy terms that have been/will be used in this thesis.

1.2.1 Variable Star

A variable star is a star whose brightness (or magnitude), as seen from Earth, fluctuates. This variation in light can be caused by a change in emitted light or by something blocking the light from reaching Earth. There are two different classifications for variable stars: intrinsic variables and extrinsic variables. Intrinsic variables are stars whose luminosity changes periodically because the star is pulsating or physically expanding and contracting. Extrinsic variables are stars whose changes in magnitude are due to a change in the amount of light able to reach Earth, i.e. something is physically between the Earth and the star, blocking the light.

1.2.2 δ Scuti Variable Star

A δ Scuti variable star is an intrinsic variable star whose brightness changes periodically. They tend to have periods on the order of 0.01 to 0.2 d (0.24 to 4.8 hrs) and amplitudes of 0.003 to 0.9 magnitudes (mag). They also tend to have many superimposed periods that combine to form complex light curves. The spectral type of δ Scuti variables is usually between A0 and F5. Spectral types are explained in Section 1.2.3.

Table 1.1. Spectral type characteristics. Values adopted from Carroll & Ostlie (2006).

Spectral Type	Color	Temperature Range (K)
O	Blue	30,000-60,000
B	Blue	10,000-30,000
A	Blue-white	7,500-10,000
F	White	6,000-7,500
G	Yellow-white	5,000-6,000
K	Orange	3,500-5,000
M	Red	2,700-3,500

1.2.3 Spectral Type

The spectral type of a star classifies it based on its spectral characteristics. It is a short code that summarizes the temperature, and therefore ionization state, of the photosphere of a star. Stars are classified using the O, B, A, F, G, K, M sequence, with the hottest stars being O type stars and the coolest stars being M type stars (see Table 1.1). Each letter class is further subdivided using the digits 0 through 9, 0 being the hottest in the letter class and 9 being the coolest (i.e. an A0 star is hotter than an A9 star).

1.2.4 Right Ascension and Declination

Right Ascension (RA) and Declination (Dec) are spherical coordinates used in the equatorial coordinate system. In astronomy, this coordinate system is used to specify the positions of celestial objects. It is designed to move with the spherical shape of sky as the Earth rotates so the coordinates of a celestial object are not continuously changing over time, nor do they change with respect to where you are on Earth. Right Ascension (symbol: α_{2000}) measures the angular distance of an object eastward along the celestial equator (the projection of the Earth's equator onto the sky) from the

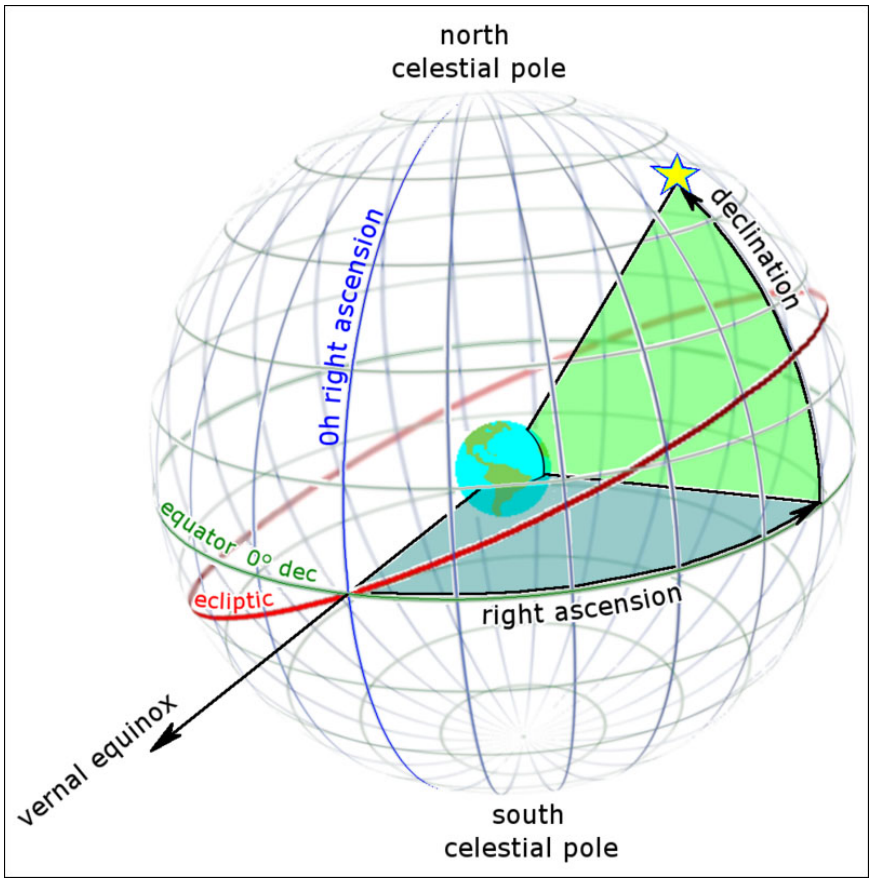

Figure 1.1 Depiction of the equatorial coordinate system from King (Accessed April 9, 2021). Note that, in this image, the red circle traces the path of the Sun through the sky, called the ecliptic. Right Ascension is measured from the vernal equinox and Declination is measured from the equator.

vernal equinox (where the path of the Sun intersects the celestial equator) to a line passing through the object, the north pole, and the celestial equator. RA is typically measured in hours, minutes, and seconds instead of degrees. Declination (symbol: δ_{2000}) measures the angular distance of an object perpendicular to the celestial equator, with north of the celestial equator being positive and south of equator being negative. For example, the declination of the celestial north pole, celestial equator, and celestial south pole is +90°, 0°, and -90°, respectively. Figure 1.1 illustrates the equatorial coordinate system.

1.2.5 Photometry

Photometry is the science of measuring light in terms of apparent brightness. It involves counting the amount of photons received from a target based on the pixel values of your light frames. Larger pixel values mean more photons were received, corresponding to a brighter object.

Differential photometry is the measurement of the difference in brightness between two objects. For variable star research, the basic idea is to measure the photons, or flux, from as many stars in the field of view as desired, then select a group of stable, non-pulsating stars as comparison stars. We take an average flux value for the ensemble and subtract it from our target star value, allowing us to calculate the relative flux coming from the target star. If the apparent magnitudes of the comparison stars are known, they can be used to determine the apparent magnitude of the target star.

1.2.6 Spectroscopy

Spectroscopy is the study of the absorption and emission of light and other radiation by matter, as related to the dependence of those processes on the wavelength of the radiation. Because the energy levels of atoms are quantized, the absorption and emission of light only occurs at specific wavelengths. In astronomy, spectroscopy is the technique of splitting light into its constituent wavelengths to produce a spectrum in order to see the absorption and emission lines of celestial objects. It is by studying these spectral lines that we are able to classify stars and deduce some of their physical properties.

1.2.7 Double-lined Spectroscopic Binary

A double-lined spectroscopic binary is a binary star system whose stars are too close together to be resolved separately. The combined spectrum of both stars shows the specific spectral line of an element twice. The two different wavelengths implies a difference in Doppler shift. Observations of

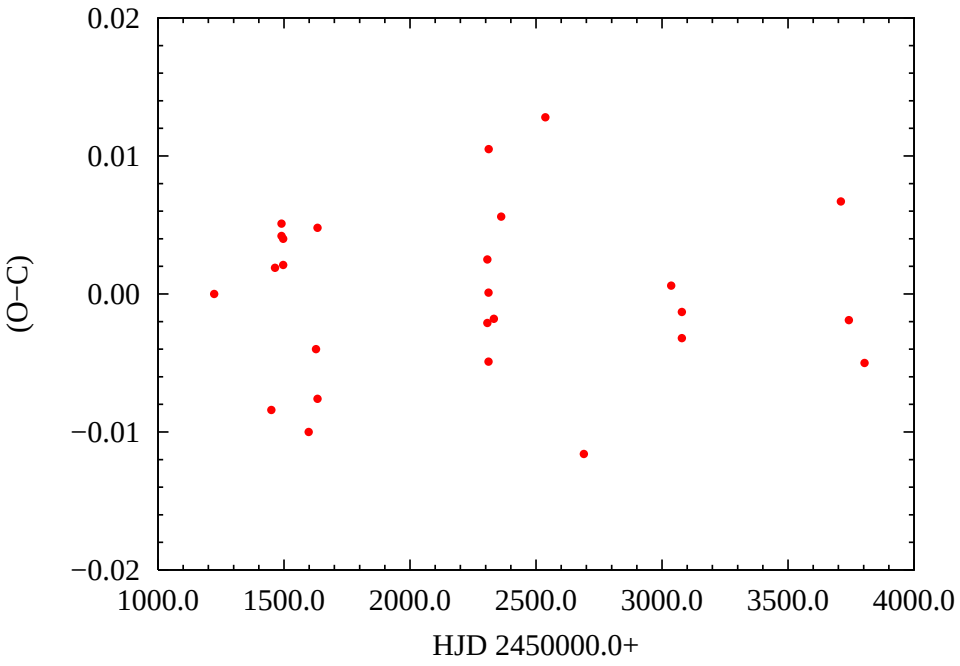

Figure 1.2 Example O-C from Hintz & Brown (2007), used with permission from the author. Note the desired trend: a scatter plot centered on zero.

double-lined spectroscopic binaries show a line that sometimes has one peak and sometimes has two peaks, changing cyclically.

1.2.8 O-C Diagram

An O-C ("O minus C" or "observed minus calculated") diagram is a useful tool for finding period changes. It is based on the idea that if a star is perfectly periodic, then every period is exactly the same. Therefore, by comparing when the observed peaks of a light curve occur to when we calculate they should occur, we can determine if the star has undergone any period changes. The desired trend for O-C diagrams is a scatter plot centered on zero. Any slope, either positive or negative, indicates an incorrect period and any discontinuity indicates a change in period. A sinusoidal trend could indicate the presence of a stellar companion. An example O-C diagram is shown in Figure 1.2.

1.2.9 Signal-to-Noise Ratio

Signal-to-noise (S/N) ratio is the ratio between the desired power of a signal and the undesired power of the background noise. A ratio higher than 1 indicates more signal than noise. A high S/N ratio is desired when observing stars and extracting frequencies from light curves.

1.2.10 Julian Date and Heliocentric Julian Date

A Julian date (JD) is the number of Julian days (24 hour days) since the beginning of the Julian period plus the fraction of a day since the preceding noon in Universal Time. JD is expressed as a Julian day integer count plus the decimal fraction of a day. Astronomers measure the passage of time in Julian days so as to not have to deal with the messiness of leap years. Heliocentric Julian date (HJD) is the JD corrected for differences in the position of the Earth with respect to the Sun.

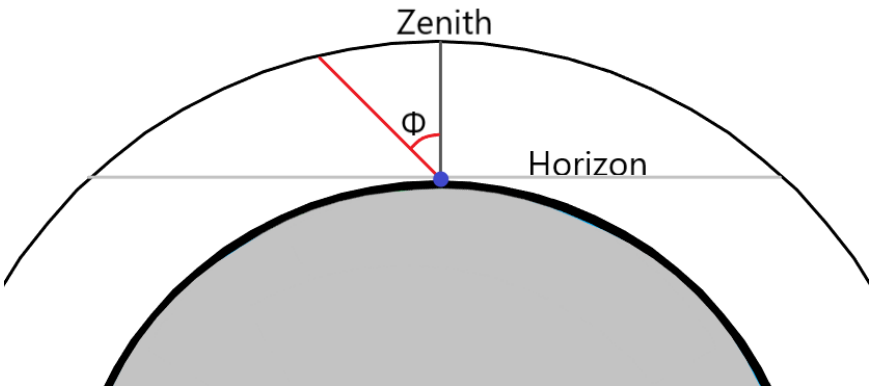

Figure 1.3 Graphic of how airmass, or the amount of air through which celestial objects are being observed, changes depending on the angle with respect to the zenith.

1.2.11 Airmass

In astronomy, airmass is the amount of the atmosphere one is looking through when observing from the Earth. Looking straight up at 90° to the surface of the Earth (the zenith) is equivalent to one airmass. Airmass increases as the angle between the target and the zenith increases, with a maximum value at the horizon. This can be seen in Figure 1.3. Knowing the airmass through which one is observing is vital because the atmosphere scatters and absorbs light. The more air light from celestial objects passes through, the less light is received. Our general practice is to not observe through more than two airmasses. This translates to not observing objects after they fall below 30° above the horizon.

1.3 History of GW Draconis

The δ Scuti variable GW Draconis (other identifiers: HIP 87541, GSC 04573-01295, TYC 4573-1295-1, AAVSO 1757+77, SAO 8960; coordinates: $\alpha_{2000} = 17^{\mathrm{h}}53^{\mathrm{m}}04.08^{\mathrm{s}}$, $\delta_{2000} = +77°23'26.5''$) is a variable star in the constellation Draco. It was found to be variable by the *Hipparcos* satellite (Perryman et al. 1997). It has a reported parallax of 3.00 ± 0.74 milliarcseconds (mas) (van Leeuwen et al. 1997), a period of 0.2524 d, a H_p magnitude range of 9.320 to 9.382, and a reported spectral type of F2 (Duerbeck 1997). GW Dra was identified as a δ Scuti variable by Kazarovets et al. (1999). A revised period of 0.1262 d was later published, along with a mean visual magnitude of 9.28 (Rodríguez et al. 2000). A radial velocity of -20.147987 ± 6.319073 km $\cdot$ s^{-1} and a parallax of 2.708923 ± 0.029712 mas were reported in the *Hipparcos*-2 catalogue (van Leeuwen 2007). Pribulla et al. (2009) published a period of 0.126184 d and a rotational velocity of <15 km $\cdot$ s^{-1}. GW Dra was excluded from a δ Scuti variable survey in 2017 because they suspected it of being a double-lined spectroscopic binary (Kahraman Aliçavuş et al. 2017).

Chapter 2

Methods

In this chapter we discuss the methods used for extracting useful information from astronomical data with the purpose of characterizing GW Dra by its period, spectral type, radial and rotational velocity, and possibility of a stellar companion. In Section 2.1 we provide details about the telescopes used in collecting both photometric and spectroscopic data on GW Dra. Section 2.1.1 addresses the setup procedures for the robotic telescopes on the observation deck of the Orson Pratt Observatory (hereafter OPO) here at Brigham Young University. In Section 2.2 we describe the process of data reduction. Section 2.3 details the procedure followed for doing differential photometry. Section 2.4 describes the process of analyzing the obtained period for accuracy and stability. Section 2.5 describes the procedures used for performing spectroscopy. A report of the challenges faced in this research project is presented in Section 2.6.

2.1 Telescopes

Several different telescopes and telescope focus/CCD combinations were used over the course of the 20 year campaign. OPO telescopes used for photometric observations include the 0.4-m David Derrick Telescope (hereafter DDT; this telescope has been replaced as of Winter 2020), a 200-mm

Vixen VMC200L, and a 250-mm Takahashi Mewlon-250. Photometric observations of GW Dra were done using the Johnson *BVRI* filters, though only the *V* filter was used for most nights. Thus, our analysis will only be done on data taken in the *V* filter. A summary of the telescopes and focus/CCD configurations used is given in Table 2.1.

Spectroscopic observations were secured at the Dominion Astrophysical Observatory (hereafter DAO) using the 1.2-m McKellar Telescope with the Coudé spectrograph utilizing the 3231 grating. This grating provides 40.9 Å·pixel^{-1}. Using the Site4 CCD with 15 μm pixels gives 0.614 Å·pixel^{-1}. The 4096 pixels along the dispersion axis means obtained spectra will cover a range of about 2500 Å.

2.1.1 Setup Procedure

To set up a telescope on the observation deck, we first connect it to the appropriate software. We use MaxImDL to connect to the telescope cameras and begin cooling the CCD chip to -25°C. While the CCD is cooling, we connect the telescope to TheSkyX, a program that allows us to control the telescope mount. We tell the telescope to go to a preset "home" position to check that the telescope is pointing where we tell it to. We then connect the first two programs to CCDAutoPilot, a software that allows us to program in a night of targets and calibration frames. Within CCDAutoPilot, we are able to see when a target rises and sets and what time is best to start observing based on civil, nautical, or astronomical twilight. We can choose which filter we wish to observe in, set the exposure time, and populate our list of targets for the night. When done, the software should be able to run the telescope and gather data all night, weather permitting.

Table 2.1. Telescope and CCD Specifications

Telescope	CCD	pixel size (μm)	Plate Scale ($''$/pixel)	Array Size (pixels)	Years
DDT Cassegrain	Apogee Ap8p	24	0.98	1024 x 1024	2001-2003
DDT Newtonian	Apogee Ap47p	13	1.65	1024 x 1024	2003
DDT Newtonian	Meade Pictor 416	9	1.14	768 x 512	2000-2002
DDT Cassegrain	SBIG ST-1001	24	0.98	1024 x 1024	2006-2007, 2011
DDT Newtonian	SBIG ST-10	6.8	0.86	2184 x 1472	2007
DDT Newtonian	SBIG STX-16803	9	1.14	4096 x 4096	2017
Vixen VMC200L	FLI ML3200	6.8	0.72	2184 x 1472	2018-2019
Takahashi Mewlon-250	FLI ML8300	5.4	0.37	3326 x 2504	2019

2.2 Data Reduction

In astronomy, we want to know the exact amount of electrons in each pixel of a CCD chip because every photon is important when looking at faint objects. Data taken using CCD cameras thus require some processing first before you can extract useful information. This processing is called data reduction and is done by applying the correct calibration frames to the corresponding light frames, where light frames is referring to pictures of the target we wish to study. Calibration frames are typically included in a night of observing and are vital in obtaining good data because they help eliminate the three different sources of noise inherent in CCD cameras. There are three different types of calibration frame, one for each source of noise: zero/bias, dark, and flat frames. Each type of calibration frame is only usable on light frames taken within roughly the same week, after which new calibration frames must be taken. Our general practice is to take calibration frames every night we observe, conditions permitting.

Zero or bias frames are taken with the shutter closed and with a zero second exposure time (hence the name "zero"). Every CCD chip prefers to operate with a preset amount of electrons in

each pixel (hence the name "bias") so as to avoid the possibility of negative pixel values. A zero frame allows us to capture what this offset for any given CCD. Zero frames also capture read-noise from the electronics and amplifiers inside CCD chips. We can then use these zero frames to remove these biases from our light frames and get a better idea of how many photons we are actually receiving from a given target.

Dark frames are taken with the shutter closed and with an exposure time matching that of a given light frame. This captures what the pixels on the CCD look like after a certain time without being exposed to light. Because the CCD is powered by a current, electrons from the current can be excited and captured by a pixel. This source of noise, called a dark current, is usually due to thermal excitation and is the reason why we cool CCDs before using them to take data. However, even at -25°C this dark current is still significant. Thus, dark frames allow us to determine the dark current present in our CCD after a given time to later remove this bias from our light frames.

Flat frames are filter specific and are taken only under certain conditions. In order to take a proper flat frame, the telescope must be pointed at a source with uniform surface brightness. Our flat frames are taken at either dusk or dawn, when the the sky directly above has a nearly uniform brightness from the sun being just below the horizon. Because not all pixels are the same, each pixel will have varying sensitivity to light. Flat frames expose the entire CCD to the same amount of light per pixel, allowing us to see the difference in sensitivity per pixel, which we can then correct for in our light frames.

Over the 20 years of observing GW Dra, a total of 71 nights of photometric data were obtained. Each individual night was reduced separately using a collection of software written at the National Optical Astronomy Observatory (NOAO) called Image Reduction and Analysis Facility (IRAF). Within IRAF, additional information, such as JD/HJD and airmass, was added to the headers of each light frame. We stacked all zero frames for a given night into a single image, which we then subtracted from each dark frame to isolate only the dark bias on those frames. We stacked all dark

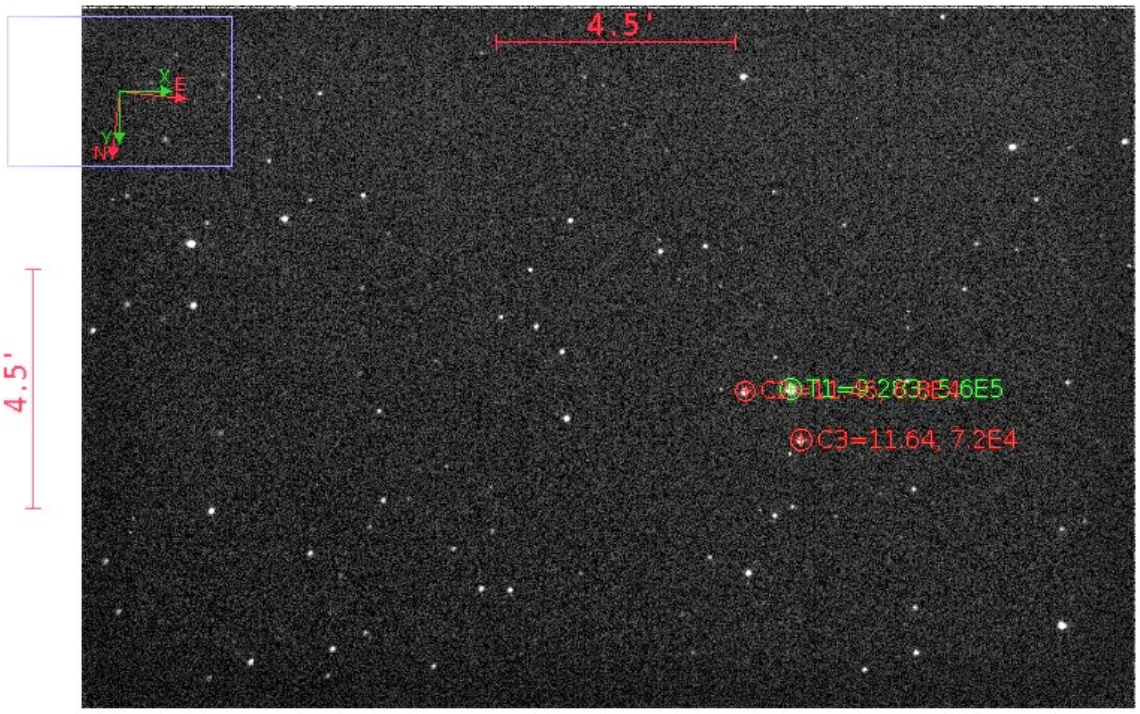

Figure 2.1 AstroImageJ frame of GW Dra (labeled T1), the surrounding star field, and two comparison stars (labeled C2 and C3, respectively).

frames into a single image, then subtracted both the combined zero and combined dark images from the flat frames to single out the flat bias in those frames. We then stacked the flat frames into a single image. These master zero, dark, and flat images were then ready to be applied to our light frames. We subtracted the zero and dark images from our light frames and then divided our light frames by the flat image. This effectively eliminated these three sources of bias from each light frame without accounting for a single source more than once. All observations were reduced using these standard IRAF procedures.

2.3 Differential Photometry

For GW Dra, we took the reduced light frames and uploaded them into AstroImageJ (Collins et al. 2017), hereafter AIJ. Each night was done individually. We identified our target star, as well as our comparison stars, and placed apertures around them. An example frame is shown in Fig. 2.1. We entered in the apparent visual magnitudes for our comparison stars, 11.46 and 11.64 for C2 and C3, respectively. These apertures were then used by AIJ to count the pixel values for each star and, based on the apparent magnitudes of our comparison stars, calculate the apparent magnitude of GW Dra in each light frame. We used AIJ to plot the light curves of GW Dra and our comparison stars. This allows us to check the stability of the comparison stars and the variability of GW Dra, as well as discern which nights of data are usable. Many different factors can cause a night to be unusable, though the most common offenders are clouds obscuring a target or comparison star mid-observation for an extended period of time or not enough time being allotted to observing a target, resulting in too few data points for a given night. An example of a usable night of data with a prominent light curve graphed in AIJ is shown in Fig. 2.2, clearly showing the variability of GW Dra and relative stability of the comparison stars. From 71 nights of data, only 39 were usable. From AIJ, we downloaded a spreadsheet for each usable night containing all the information available in each frame.

2.4 Period Analysis

A list of times and magnitudes was extracted from the spreadsheets created by AIJ, which were then imported into Period04 (Lenz & Breger 2005) for period analysis. A Fourier analysis was performed to extract the frequency composition of GW Dra and determine its period. The results of the Fourier analysis could then be used to effectively model the light curve of our system using the

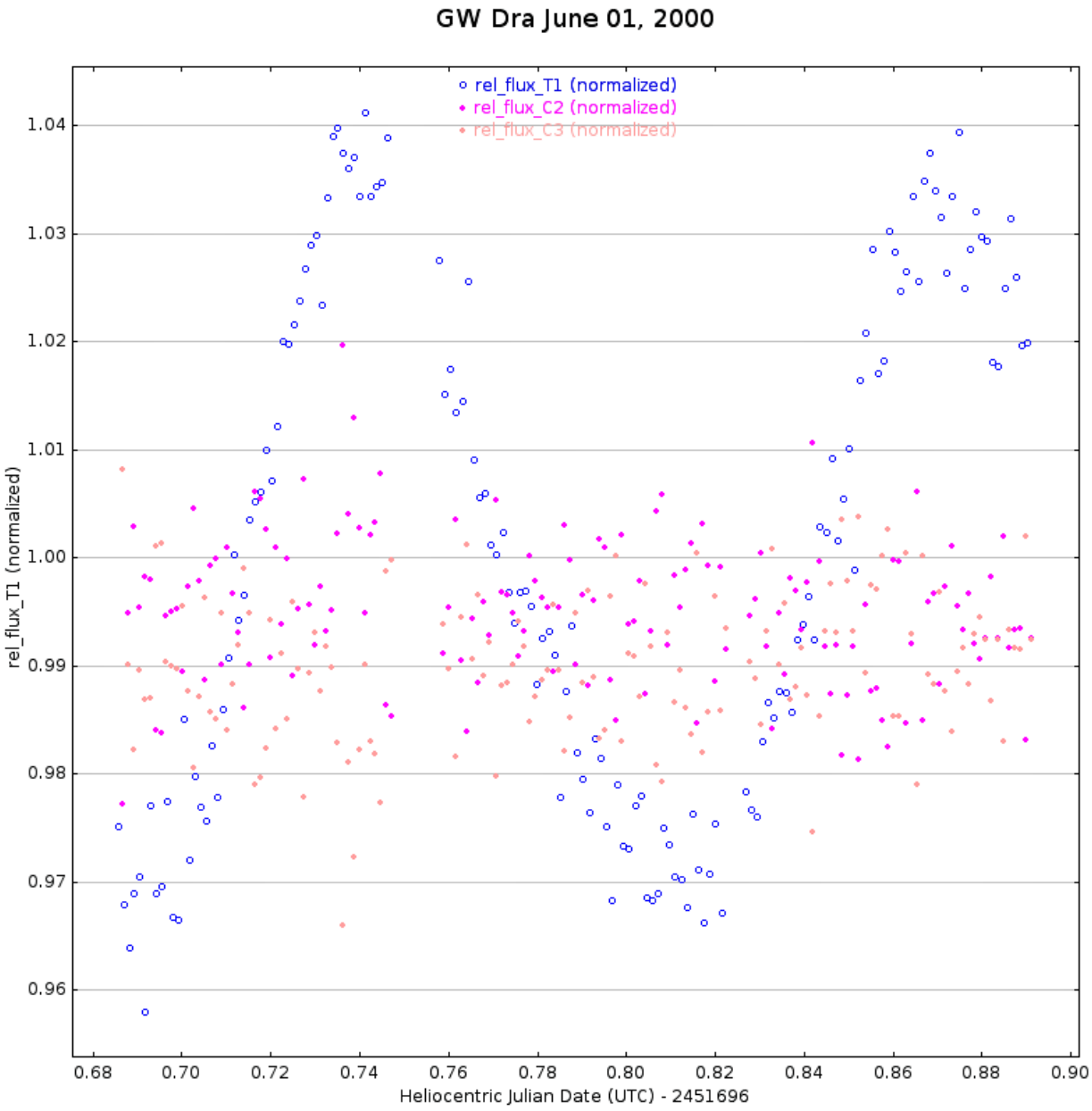

Figure 2.2 Example light curve of GW Dra in AstroImageJ of relative flux vs Heliocentric Julian Date (HJD) measured in days. The blue dots show the change in flux coming from GW Dra over time. The purple and salmon dots show the flux of the comparison stars. Note the clear variability of GW Dra and the stability of the comparison stars.

equation

$$F = Z + \sum A \sin(2\pi(\Omega t + \phi)), \tag{2.1}$$

where F is flux, Z is a set zero point, A is the amplitude, Ω is the frequency, and ϕ is the phase. These same lists were then imported into the software package Peranso (Paunzen & Vanmunster 2016) to determine the times of maximum light by using a polynomial fit to each maximum and solving for the zero slope point. Using the calculated period and the times of maximum light, we compared when the peaks of the light curves should occur, based on the period, to when they actually occur, based on our observations. The equation describing when the peaks in the light curve of a variable star should occur is an ephemeris equation

$$HJD_{max} = Z + P * E, \tag{2.2}$$

where HJD_{max} is the time of maximum light, Z is the zero point, P is the period, and E is the cycle number. Subtracting the observed times of maximum light from those calculated using Eq. (2.2) and plotting the resulting values vs. HJD, we created an O-C diagram. This O-C diagram was then analyzed to see if the calculated period is accurately representing the data, if the period has been stable over the 20-year range, and if there are signs of a stellar companion.

2.5 Spectroscopy

Spectra can be reduced in IRAF by applying the pertinent calibration frames, similar to those used to reduce photometric data. Zero/bias and flat frames are necessary for spectra, but not dark frames. Telescopes that are equipped to take spectra typically cool their CCD chips to such a low temperature that the dark current becomes negligible, eliminating the need for dark frames. Wavelength calibration of spectra is typically done with an FeAr comparison arc. Once reduced, we can use the method detailed in Joner & Hintz (2015) to compare the spectra taken with different

filters and determine Hα index measurements for each night of data. Once determined, these measurements can then be converted into effective or surface temperature through the relation

$$T_{\text{eff}} = \frac{5040 \text{ K}}{(-162.627 * H_{\alpha}^{4}) + (1751.335 * H_{\alpha}^{3}) + (-7063.688 * H_{\alpha}^{2}) + (12644.249 * H_{\alpha}) - 8473.302} \tag{2.3}$$

where H_{α} is the Hα index. Using the surface temperature, we can determine the spectral type of the star.

The width of spectral lines can be analyzed to calculate the rotational velocity of the star. Spectral line width is caused by the Doppler shift from the rotation of the star, where the side of the star moving towards us will be blue shifted while the side moving away will be red shifted. The wavelengths of spectral lines can also be measured to determine the radial velocity of the star because the movement of the star towards or away from us will shift the entire spectra accordingly. Spectra can also be analyzed to determine the existence of stellar companions.

2.6 Challenges

Several challenges were encountered over the course of this project. The first and most notable was a disparity in how well our calculated period lined up with our observational data. The data seemed to have a piece missing, a gap sometime between April and June 2000 where GW Dra appeared to have stopped pulsating for an hour before resuming its normal pulsations. This challenge was overcome when we realized that around that same time someone had manually changed the clock on the telescope for daylight savings instead of letting it change by itself, putting our data off by one hour exactly. Adding in this lost hour filled the apparent hole in the data.

Another challenge was faced when we realized AIJ had not properly extracted the HJDs from the headers of our files. HJDs are important for more accurate analysis of what time events occur, so our analysis was lacking without these vital dates. This meant having to go back and re-reduce

all the data to properly extract the HJDs for each usable night. Resolving this challenge did yield some unexpected positive results as extra nights of data we did not know existed were found and some nights previously classified as unusable became usable.

Chapter 3

Results and Conclusions

In this chapter we discuss the results of the photometric and spectroscopic analyses of our data. In Section 3.1 we report on the frequency composition of GW Dra, determine its period, and analyze the period for stability. Section 3.2 is a report of the results of our spectroscopic analysis. A summary of our results is given in Section 3.3.

3.1 Photometric Analysis

Fourier analysis yielded a fundamental frequency of 7.92482261 d^{-1}, several other unique frequencies, and some subharmonics, but no harmonics of orders higher than the fundamental. Within Period04, we extracted over 20 unique frequencies and subharmonics from the combined data. Because we were dealing with data taken over two decades, extremely low frequencies corresponding to periods of one year to several years were inevitable. However, these frequencies are not pertinent to the star being observed and can be ignored as artefacts of the data. We therefore examined these 20 frequencies for relevance and discarded those we determined to likely be inherent in the data or if the S/N ratio was too low. For the purposes of our research, a S/N ratio greater than 4.0 was considered usable. The resulting nine significant frequencies of GW Dra can be seen in Table 3.1,

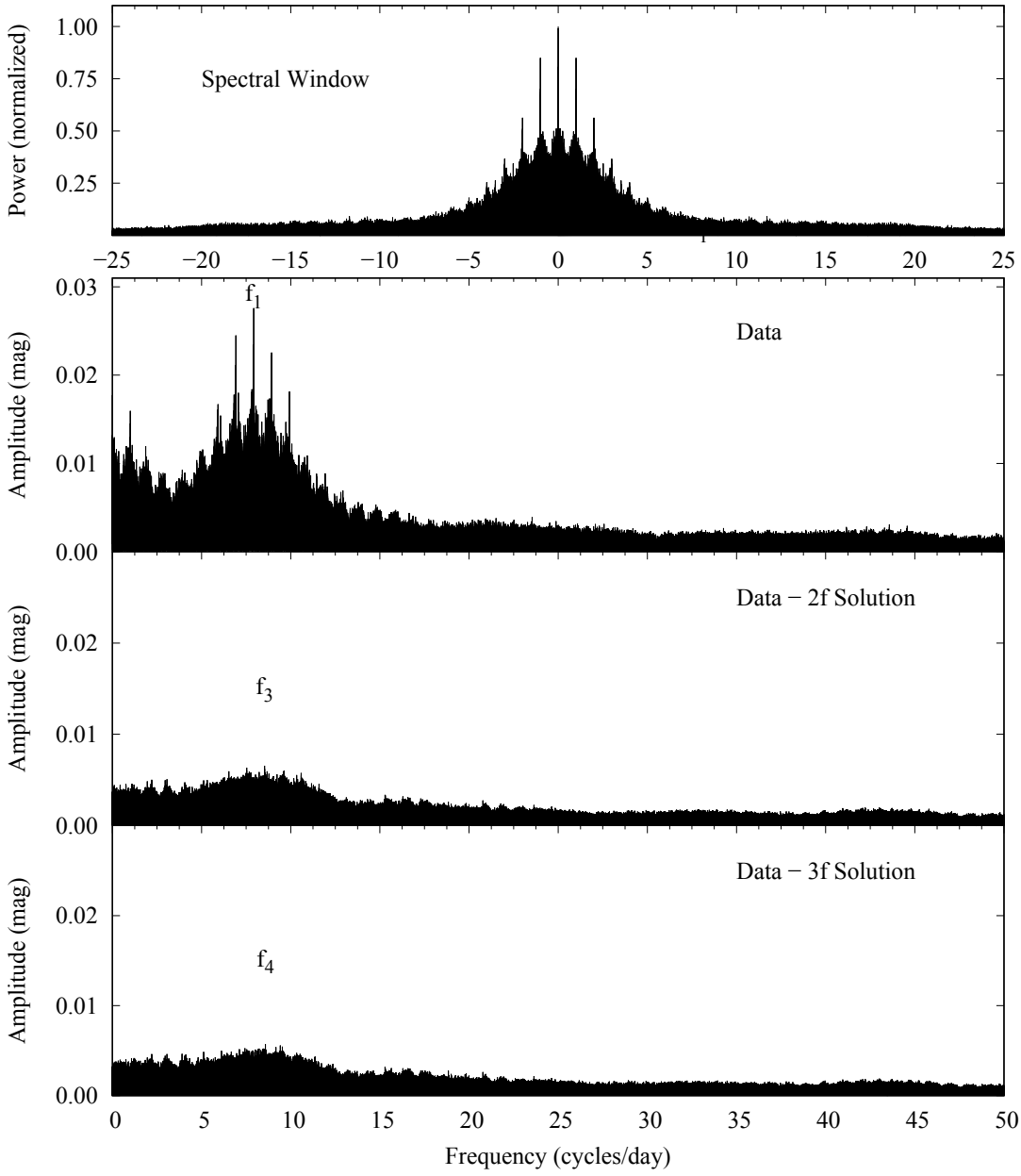

Figure 3.1 Spectral window and frequency spectra of the first three significant frequencies from Table 3.1. The 2f solution is the resulting frequency spectra without f_1 and f_2 contributions (f_2 not given in Table 3.1 because it was determined to be an artefact of the data and discarded). The 3f solution is the resulting spectra without f_1, f_2, and f_3 contributions. The spectral window power is normalized and unitless. The x-axis units are the same for all four windows.

Table 3.1. Frequency content of GW Dra

ID	Frequency (cycles d^{-1})	Freq. σ (cycles d^{-1})	Amplitude (mag)	Phase	S/N
f_1	7.92482261	8.776524158e-07	0.02561791	0.88873031	28.70881
f_3	8.53109977	2.627739451e-06	0.00855626	0.52305251	10.13118
f_4	8.57945382	2.836445735e-06	0.00792669	0.61922367	9.4219
f_5	6.32240221	3.271562802e-06	0.00687244	0.03761426	7.34914
f_6	5.11441268	4.500380618e-06	0.00499594	0.81463261	5.03473
f_7	9.52690831	3.975018437e-06	0.00565623	0.63543936	7.33911
f_{11}	10.1497854	6.092941873e-06	0.00369011	0.34917730	5.13996
f_{16}	14.1291740	8.962188361e-06	0.00250872	0.11331227	4.1659
f_{20}	17.7872539	8.606069058e-06	0.00261253	0.96603866	5.03437

along with the frequency error, amplitude of the signal, phase, and S/N ratio. The spectral window and frequency spectra of some of the significant frequencies can be seen in Fig. 3.1 and show this lack of harmonics. These frequencies are labeled as f_1, f_3, and f_4 respectively. Note that f_2 is neither included in Table 3.1 nor shown in Fig. 3.1 because it was determined to be an artefact of the data and discarded. This lack of harmonics and prominence of unique frequencies unrelated to the fundamental indicate that GW Dra is multiperiodic.

Using Eq. (2.1) and the results of the Fourier analysis, we were able to plot a line of best fit over all nights of usable data. This is shown in Fig. 3.2. From the graph, it is clear that our Fourier analysis was able to produce a model that fit the data fairly well. Each night is plotted in the same apparent visual magnitude window. Thus, Fig. 3.2 also shows the multiperiodic nature of GW Dra, apparent in the varying amplitude of the light curves in time. As previously stated, GW Dra had a reported period of 0.2524 d with revised periods of 0.1262 d and 0.126184 d published later. Our calculated fundamental frequency (f_1) corresponds to a period of 0.126186 d, in excellent agreement with these revised periods. From our nights of usable data, we obtained 44 times of maximum

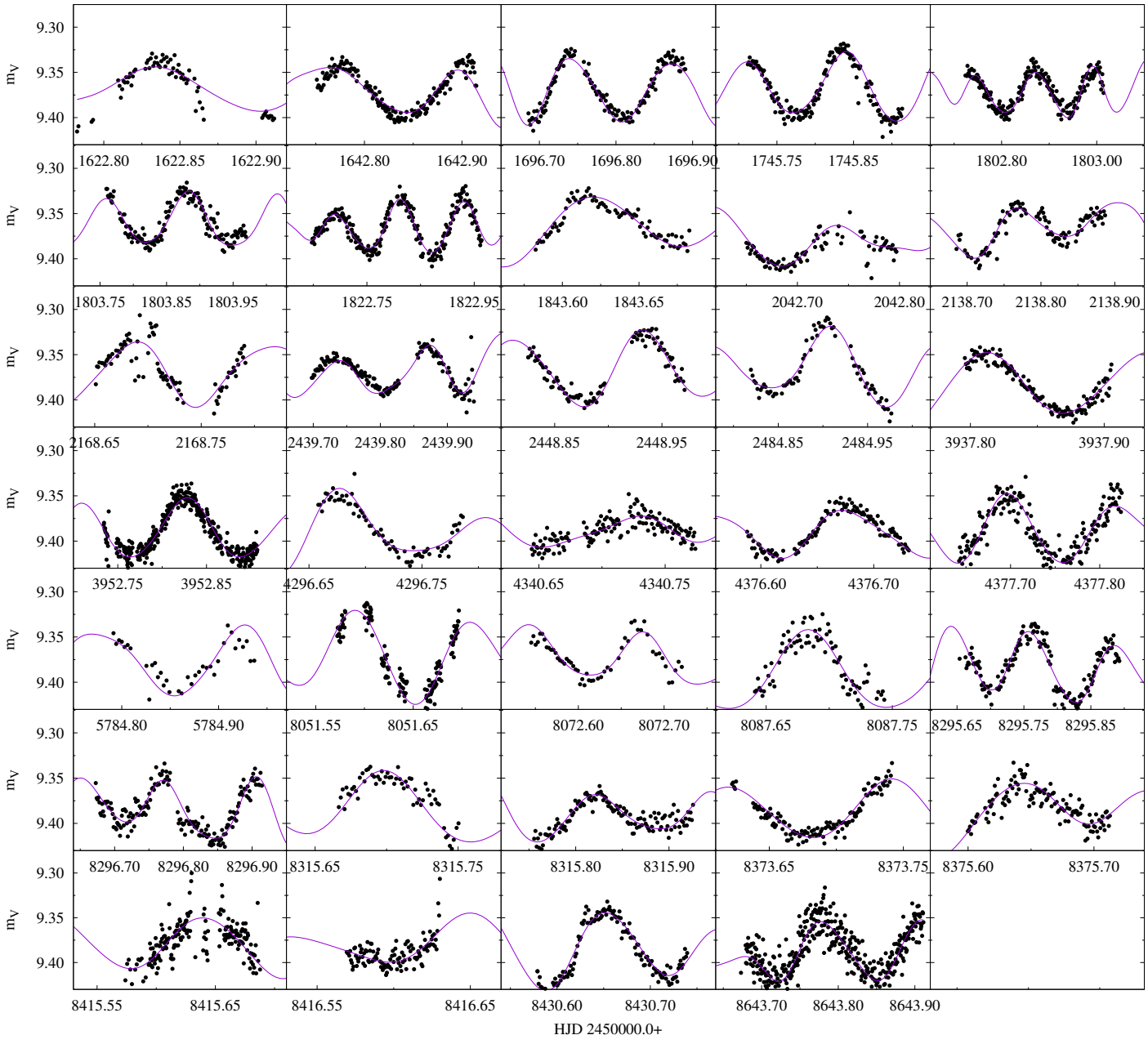

Figure 3.2 All nights of usable data of GW Dra overlaying a line of best fit. Each night is shown in the same apparent visual magnitude (m_V) window. HJD 2450000.0+ is measured in days with the first three digits subtracted off for sake of clarity; m_V is in magnitudes.

light. These can be found in Appendix A (see Table A.1). Using the information in Table A.1, our calculated period, and Eq. (2.2), we generated the O-C diagram shown in Fig. 3.3. Our O-C has no discernible trend, so we conclude that our period accurately represents the data and has been stable for the past 20 years. Absence of a sinusoidal trend in the O-C also indicates that GW Dra may not have a stellar companion. The wide vertical scatter (compare with the vertical scale of Figure 1.2) could be due to a multiperiodic nature.

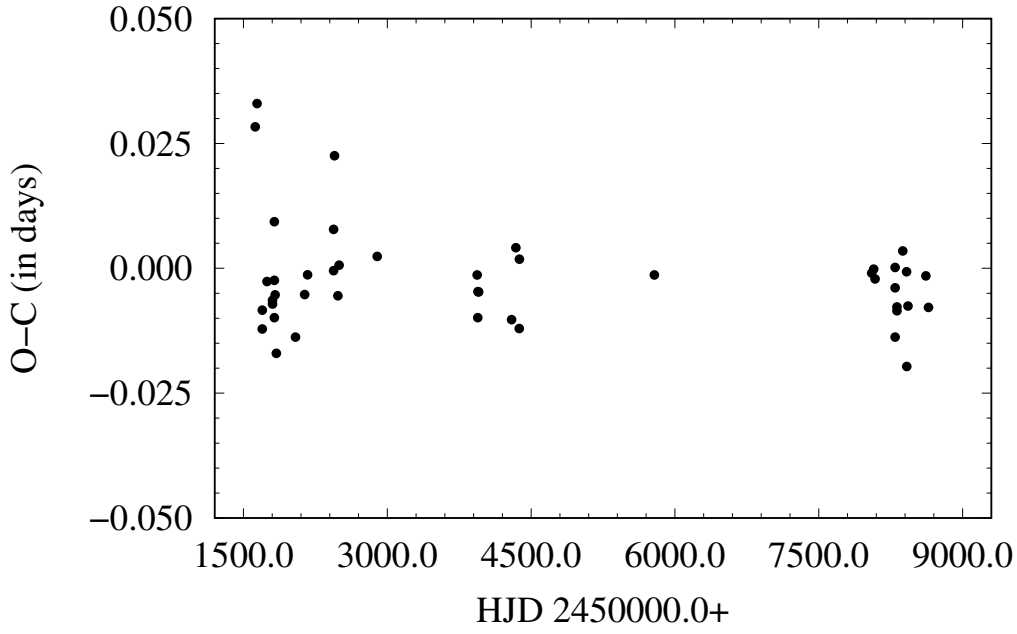

Figure 3.3 O-C diagram for GW Dra constructed from the period, times of maximum light, and Eq. (2.2). No obvious trend is seen, indicating that the period of GW Dra has been stable over the 20 years of observations and may not have a stellar companion. HJD 2450000.0+ is measured in days with the first three digits subtracted off for sake of clarity.

3.2 Spectroscopic Analysis

Analysis of each night we obtained spectra for GW Dra yielded several Hα index measurements. These measurements were converted into temperature using Eq. (2.3) and yielded a surface tem-

perature range of 7470 to 7770 K, putting GW Dra in the temperature range between the A and F spectral types. With a midpoint surface temperature of 7620 K, GW Dra is most likely an A8, A9, or F0 star. This disagrees with the F2 spectral type reported by Duerbeck (1997).

As previously noted, GW Dra was rejected from a δ Scuti variable survey because it was suspected of being a double-lined spectroscopic binary. Analysis of the spectra obtained on GW Dra does not show spectral lines from two stars as would be expected for a double-lined spectroscopic binary. We therefore assert that GW Dra is not a double-lined spectroscopic binary.

3.3 Conclusion

We studied 20 years of data on the δ Scuti variable GW Draconis. We found a period of 0.126186 d, in agreement with the revised published periods of 0.1262 d and 0.126184 d. The O-C diagram for GW Dra shows no trend, indicating that our calculated period is accurate and has been stable since the original observations in 2000. Frequency analysis of GW Dra yielded several unique frequencies and some subharmonics but failed to extract higher order harmonics. The large vertical scatter in the O-C diagram and many unique frequencies indicate that GW Dra is multiperiodic. Spectral analysis yielded a surface temperature range of 7470 to 7770 K with a midpoint of 7620 K, making GW Dra most likely an A8, A9, or F0 star. This disagrees with the previously published spectral type of F2. Spectra do not show spectral lines from two stars, as expected in a double-lined spectroscopic binary. Therefore, we do not consider GW Dra to be a double-lined spectroscopic binary.

Appendix A

Table: Times of Maximum Light

Due to the large size of our times of maximum light table, we decided it was best to include it here rather than have it distract from the main body. The cycle number is the number of peaks that have occurred since our first observation in 2000; HJD 2450000.0+ is the time of the peak at the given cycle number with the first three digits of the HJD subtracted off for clarity; O-C is the difference in days from when the peaks are observed to occur and when they should occur.

Table A.1. Times of Maximum Light for GW Dra

Cycle	HJD 2450000.0+	$O-C$
0	1622.835870	0.028343
158	1642.777867	0.032985
586	1696.740247	-0.012153
587	1696.870214	-0.008372
975	1745.836031	-0.002641
1427	1802.868252	-0.006397
1435	1803.876992	-0.007143
1584	1822.695157	0.009339
1585	1822.809597	-0.002407
1586	1822.928316	-0.009874
1640	1829.746901	-0.005321
1750	1843.615647	-0.017012
3328	2042.740060	-0.013775
4089	2138.775968	-0.005253
4326	2168.685937	-0.001317
6474	2439.733850	-0.000480
6475	2439.868307	0.007791
6547	2448.968431	0.022538
6832	2484.903332	-0.005511
6927	2496.897122	0.000629
10080	2894.762670	0.002382
18346	3937.810695	-0.001332
18394	3943.859074	-0.009870
18402	3944.873747	-0.004684
18465	3952.823409	-0.004726
21190	4296.674134	-0.010279
21539	4340.727386	0.004133
21824	4376.674140	-0.012063
21832	4377.697498	0.001808
32984	5784.918282	-0.001335

Table A.1 (cont'd)

Cycle	HJD 2450000.0+	$O-C$
50947	8051.594004	-0.000956
51114	8072.667826	-0.000160
51233	8087.681964	-0.002131
52882	8295.764629	0.000166
52883	8295.876862	-0.013787
52890	8296.770035	-0.003914
53040	8315.694071	-0.007747
53041	8315.819511	-0.008492
53515	8375.643560	0.003492
53832	8415.640266	-0.000697
53848	8417.640273	-0.019663
53951	8430.649506	-0.007566
55427	8616.905783	-0.001515
55640	8643.777039	-0.007832

Bibliography

Carroll, B. W., & Ostlie, D. A. 2006, An introduction to modern astrophysics and cosmology

Collins, K. A., Kielkopf, J. F., Stassun, K. G., & Hessman, F. V. 2017, AJ, 153, 77

Duerbeck, H. W. 1997, Information Bulletin on Variable Stars, 4513, 1

Hintz, E. G., & Brown, P. J. 2007, PASP, 119, 274

Joner, M. D., & Hintz, E. G. 2015, AJ, 150, 204

Kahraman Aliçavuş, F., Niemczura, E., Polińska, M., Hełminiak, K. G., Lampens, P., Molenda-Żakowicz, J., Ukita, N., & Kambe, E. 2017, MNRAS, 470, 4408

Kazarovets, E. V., Samus, N. N., Durlevich, O. V., Frolov, M. S., Antipin, S. V., Kireeva, N. N., & Pastukhova, E. N. 1999, Information Bulletin on Variable Stars, 4659, 1

King, B. Accessed April 9, 2021, https://skyandtelescope.org/astronomy-resources/right-ascension-declination-celestial-coordinates/

Lenz, P., & Breger, M. 2005, Communications in Asteroseismology, 146, 53

Paunzen, E., & Vanmunster, T. 2016, Astronomische Nachrichten, 337, 239

Percy, J. Accessed March 3, 2021, https://www.aavso.org/variables-what-are-they-why-observe-them

Perryman, M. A. C., et al. 1997, A&A, 500, 501

Pribulla, T., et al. 2009, AJ, 137, 3655

Rodríguez, E., López-González, M. J., & López de Coca, P. 2000, in Astronomical Society of the Pacific Conference Series, Vol. 210, Delta Scuti and Related Stars, ed. M. Breger & M. Montgomery, 499

van Leeuwen, F. 2007, A&A, 474, 653

van Leeuwen, F., Evans, D. W., Grenon, M., Grossmann, V., Mignard, F., & Perryman, M. A. C. 1997, A&A, 323, L61

Index